ChemEurJ

Research Article
doi.org/10.1002/chem.202501990

Chemistry Europe
European Chemical Societies Publishing

www.chemeurj.org

$Ag_5Pd_2O_4$, a New Subvalent Silver Oxide, Obtained from Ag_2PdO_2 via a High-pressure Synthesis

Sihana Ahmedi,[a] Natalia Martynova,[a] Nico Giordano,[b] Michael Hanrath,[c] Martin Jansen,*[a, d] Maxim Bykov,*[e] and Jörn Bruns*[a]

Subvalent silver oxides, where silver exhibits an oxidation state between 0 and + 1, have traditionally been discovered serendipitously due to a lack of systematic synthesis methods and understanding of their bonding schemes. This study presents a novel, purposeful approach to synthesizing multinary subvalent silver oxides through high-pressure techniques. By subjecting the monovalent silver oxide Ag_2PdO_2 to hydrostatic pressure of ~30 GPa and laser heating at 1500 K, subvalent $Ag_5Pd_2O_4$ forms besides PdO. The crystal structure of $Ag_5Pd_2O_4$, determined via in situ single-crystal X-ray diffraction, reveals distinct layers of cationic silver aggregates and anionic oxopalladate units. Electronic structure calculations confirm the subvalent nature of silver in $Ag_5Pd_2O_4$, showing a vanished band gap and increased electron density on silver atoms. The findings pave the way for developing materials with rich magneto-electronic functionalities, owing to the interplay between subvalent silver and transition metal cations.

1. Introduction

Experimental evidence for attractive interactions between Ag^+ cations, postulated to be effective in silver-rich ternary oxides,[1] has been consolidated substantially. The similarity of the extended silver substructures encountered in such oxides to the crystal structure of elemental silver is not only restricted to short Ag-Ag separations, which approach those present in pristine silver. Moreover, the structures of the cluster-like arrangements of $(Ag^+)_n$ formed correspond to motifs as excised from the fcc structure of silver metal. This finding has encouraged to anticipate that such substructures would be suited to host excess electrons in the nominally empty and low-lying 5s and 5p bands, thus resulting in subvalent silver oxides.[1b] Indeed, a number of new compounds fulfilling this expectation have been realized (e.g., Ag_5SiO_4, $Ag_5Pb_2O_6$, $Ag_3Ni_2O_4$, Ag_5GeO_4, $Ag_7Pt_2O_7$, $Ag_{16}B_4O_{10}$).[2] All of them were discovered just by chance during systematic exploration of respective ternary silver oxide systems experimentally. The candidates realized so far are quite diverse, covering a large variety of constituents and structural features. This lack of systematics has impaired any effort made to classify the findings, to rationalize the bonding scheme, or to develop cause-effect relationships along the path of inductive reasoning.

Here, we report on subvalent $Ag_5Pd_2O_4$ as obtained from Ag_2PdO_2,[3] which features conventional valence states for all constituents, by a high-pressure reaction under simultaneous release of PdO. This discovery appears to be of far-reaching relevance, as it is indicating an option for a purposeful and generally applicable access to multinary subvalent silver oxides. The high pressure driving the reaction suggests a shrinkage of the sample volume. We attribute the dominant share of compression to silver, since the second phase formed is PdO in its ambient pressure structure. In order to check if a reduced volume is a general property of subvalent silver oxides, one can consider the volume balances of normal valent versus subvalent ternary silver compounds within the framework of the atomic volume increments according to W. Biltz.[4] The idea can be demonstrated at the example of the closely related pair of Ag_4SiO_4[5] and Ag_5SiO_4.[2d] One has to subtract the molar volume increments of Si^{4+} and 4 O^{2-} from the total molar volumes derived from the unit cell volumes. Dividing the residual volume by 4 or 5, respectively, provides the effective molar volume increment of Ag in the subvalent and normal valent compound. As a result, the volume increment of silver cations in the subvalent compound is smaller

[a] S. Ahmedi, Dr. N. Martynova, Prof. Dr. M. Jansen, PD Dr. J. Bruns
Institute of Inorganic and Materials Chemistry, University of Cologne, Greinstrasse 6, Cologne 50939, Germany
E-mail: m.jansen@fkf.mpg.de
j.bruns@uni-koeln.de

[b] N. Giordano
Deutsches Elektronen Synchrotron (DESY), Notkestrasse 85 22607, Hamburg, Germany

[c] PD Dr. M. Hanrath
Institute for Light and Materials, University of Cologne, Greinstrasse 4 50939, Cologne, Germany

[d] Prof. Dr. M. Jansen
Max Planck Institute for Solid State Research, Heisenbergstraße 1 70569, Stuttgart, Germany

[e] Prof. Dr. M. Bykov
Institute for Inorganic and Analytical Chemistry, Goethe University Frankfurt, Max-von-Laue-str. 7 60438, Frankfurt, Germany
E-mail: maxim.bykov@chemie.uni-frankfurt.de

Supporting information for this article is available on the WWW under https://doi.org/10.1002/chem.202501990

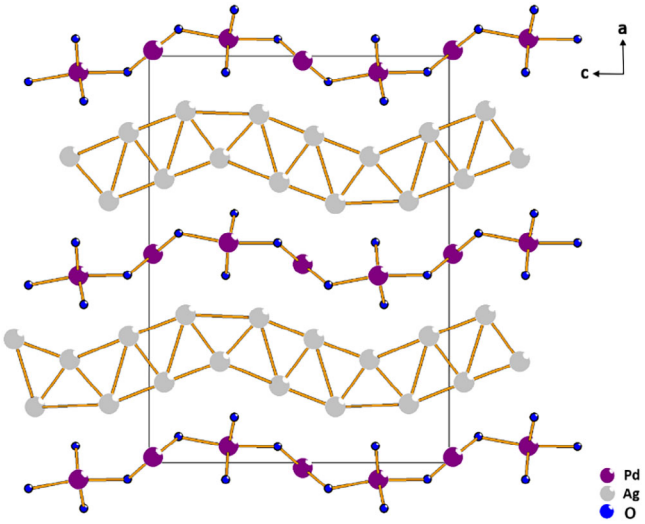

Figure 1. Ambient pressure phase of $Ag_5Pd_2O_4$ ($Cmc2_1$) in projection onto the *bc*-plane.

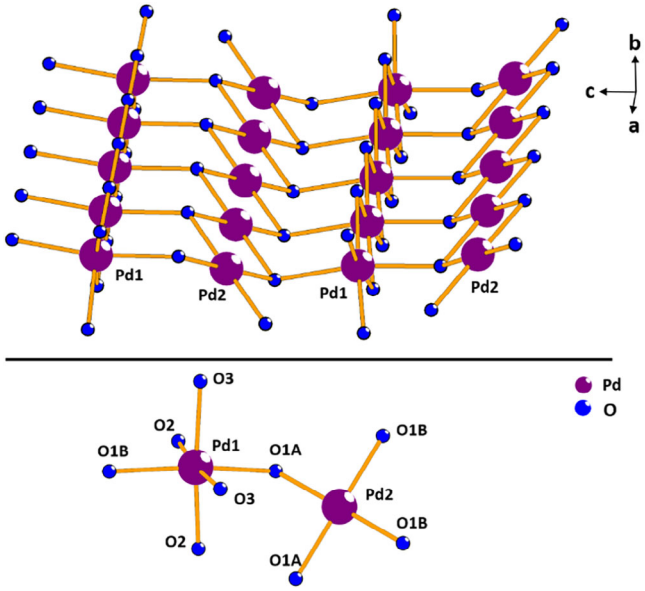

Figure 2. Top: Pd-O substructure in the crystal structure of $Ag_5Pd_2O_4$ ($Cmc2_1$); bottom: first coordination spheres of Pd1 and Pd2. The Pd-O distances [Å] are Pd1-O1A 2.01(3), Pd1-O1B 2.07(4), Pd1-O2 2.03(4), Pd1-O3 2.03(4), Pd2-O1A 2.02(3), Pd2-O1B 2.01(3).

by ~10% compared to that in the normal valent silver silicate. Since in all known subvalent silver oxides the silver substructures are contracted, such a reduced volume increment for Ag^+ appears to be a general attribute of this class of compounds, and as mentioned above, applying high-pressure techniques will open systematic synthetic approaches to subvalent silver oxides.

2. Results and Discussion

When subjected to a hydrostatic pressure of ~30 GPa in a diamond anvil cell (DAC)[6] and laser heating (T = 1500 K), Ag_2PdO_2 (Figure S1) reacts to $Ag_5Pd_2O_4$ under simultaneous formation of PdO. The crystal structures were determined and refined using single crystal intensities collected in situ on a multigrain crystal; see Supplementary Information (SI) for details. Independent of the valence assigned to palladium (+2, +4, or mixed + 2/+4), the electron count for $Ag_5Pd_2O_4$ reveals a clearly subvalent state of silver, which induces a particular crystal structure showing a conspicuous clustering and spatial separation of the anionic oxopalladate and cationic silver arrays. These substructures form undulating slabs that are stacked in an alternating fashion along the crystallographic b-axis; see Figure 1. Crystal structure refinements were performed on samples while maintaining high pressure (30.4 GPa) and after decompression. During relief of pressure, a diffusionless structural phase transition occurs, lowering space group symmetry from *Cmcm* to the maximal subgroup $Cmc2_1$ (see Figure S2), confirming that the new oxide is stable at ambient pressure as well. Details of crystal structure analyses, bond lengths, and angles are included in Supporting Information; see Tables S1–S7. For the sake of comparability with published data on interatomic separations, we first discuss the ambient pressure crystal structure.

For palladium, the valence states can be deduced from the shape and bond lengths of the first coordination spheres; see Figure 2. The square-planar coordination and the Pd-O distances of ~2.02 Å found for Pd2 are clearly indicative of its divalent state.[3,7] In contrast, Pd1 displays an approximately sixfold octahedral coordination, which is regarded a preferred environment for Pd^{4+} in oxides,[8] however, it has also been encountered in rare instances for Pd^{2+}.[9] Even though the substantial difference in published pertinent metal-oxygen bond lengths (~2.05 Å and ~2.20 Å for Pd^{4+} and Pd^{2+} in octahedral coordination, respectively) suggests the oxidation state of + 4 for Pd1. The square planar (PdO_4) as well as the octahedral (PdO_6) primary building units are linked among themselves by sharing edges in *trans* position, this way forming strands extending along [100]. The oxygen atoms of the $_\infty{}^1Pd2O_{(4/2)}$ chains serve as apical ligands completing the coordination of Pd1. The resulting 2D polyoxopalladate anion is shown in Figure 2. In accordance with the afore made assignment of charges, the chemical formula reads as $Ag_5Pd_2O_4{\cdot}3e^-$, while associating the excess electrons to the silver substructure.

The crystal structure of $Ag_5Pd_2O_4$ displays a conspicuous separation of the polyanionic and cationic substructures, which is a characteristic feature of silver-rich oxides.[1] The silver aggregates form undulating double layers extending perpendicular to the crystallographic c-axis, c.f. Figure 1; the linkage to the polyoxopalladate slabs is mediated by regular Ag-O-Pd bridges.

As a rule, regions of extended solids, where less rigid chemical bonding prevails, like, for example, dispersive interactions, shrink more strongly than those of rigid bonding when subjected to elevated hydrostatic pressure.[10] This corresponds to our present observations: silver-silver separations drop more with growing pressure than the metal-oxygen bond lengths; see Figure 3.

The coordination polyhedra around palladium slightly tilt while releasing pressure. The bond lengths and angles show commonly observed changes in response to hydrostatic

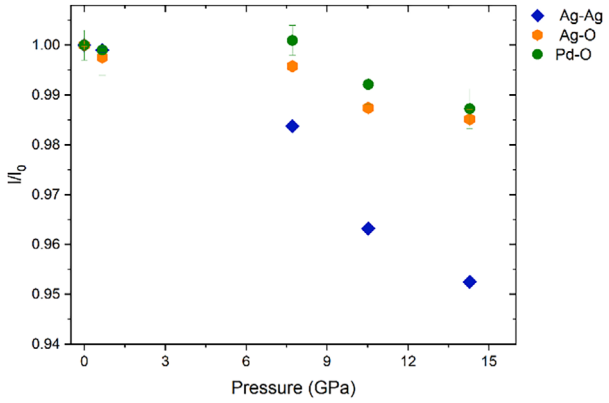

Figure 3. Relative Ag-Ag, Ag-O and Pd-O distances in Ag_2PdO_2 as a function of pressure. Data were collected on compression of Ag_2PdO_2 without laser heating.

pressure applied. The silver substructure of the high-pressure phase of $Ag_5Pd_2O_4$ is displayed in Figure 4 as an excised body.

Considering Ag-Ag separations of up to 3 Å, we identify approximately octahedral (Ag_6) entities as primary building blocks, which are linked by trans-edge sharing to form double strands as secondary building units, extending along [100]. The remaining terminal vertices connect, forming the tertiary structure, undulating double layers as shown in Figure 1 in projection along [100]. While the overall silver substructure stays unaltered during relief of pressure, a closer inspection reveals substantial changes in detail, which mainly refer to the approximately tetrahedral voids present in the silver substructure. There are two different types; one, labeled as *A* in Figure 4, results in the region of shared vertices; the second, *B*, is formed as a gusset by three adjacent, *trans*-edge-linked octahedra. These areas are considerably shrunk in the crystal structure at 30.4 GPa. Fragment *A* includes four short Ag-Ag distances of 2.67 Å, and two considerably longer ones (2.85 and 2.94 Å), rendering its overall shape rather butterfly- instead of tetrahedron-like; see Figure 4. This structural feature shares vertices to form 1D strands along [100], as accentuated in Figure 4, left, by bold rods in red. Within unit *B* we identify one very short Ag-Ag separation of 2.64 Å in length and four still rather short (2.77 Å), while the remaining one is considerably longer (2.85 Å). These subunits are connected via *cis* edges, this way generating a zigzag chain of the shortest bonds extending along [100], as emphasized by red rods in Figure 4.

We associate such shrinking of Ag-Ag separations with a kind of localization of the excess electrons in silver 5s and/or 5p bonding states. In ideal instances, where the number of shrunken regions corresponds to the number of pairs of excess electrons, semiconducting and diamagnetic ground states result.[2b,c,j,l,11] In the present case, there are six pairs of extra electrons per unit cell distributing partially over twelve contracted local units present.

In contrast, the crystal structure ($Cmc2_1$) of the decompressed sample does not show such pronounced modulations, as can be easily seen from the spread of distances between adjacent silver atoms, which is 2.81–300 Å pm compared to 2.64—2.94 Å as observed at 30.4 GPa. One may discuss the phenomena in terms of the charge density wave (CDW) concept[2j,l,12] assuming dynamic CDWs at ambient pressure, which get pinned when applying high pressure.

We analyzed the electronic structures of the two polymorphs of $Ag_5Pd_2O_4$ encountered and of Ag_2PdO_2 as a reference by DFT calculations. The computations were carried out with the Crystal 17 program suite[13] using the HSEsol[14] functional at pob-TZVP[15,16] basis set quality with a 16,16 k-space grid. Supplementary spin unrestricted calculations show no open shell character of the $Ag_5Pd_2O_4$ system. Additional calculations using the PBESol[17] functional show smaller gaps but do not affect the principle findings of the following discussion. Figure 5 displays the resulting densities of state (DOS).

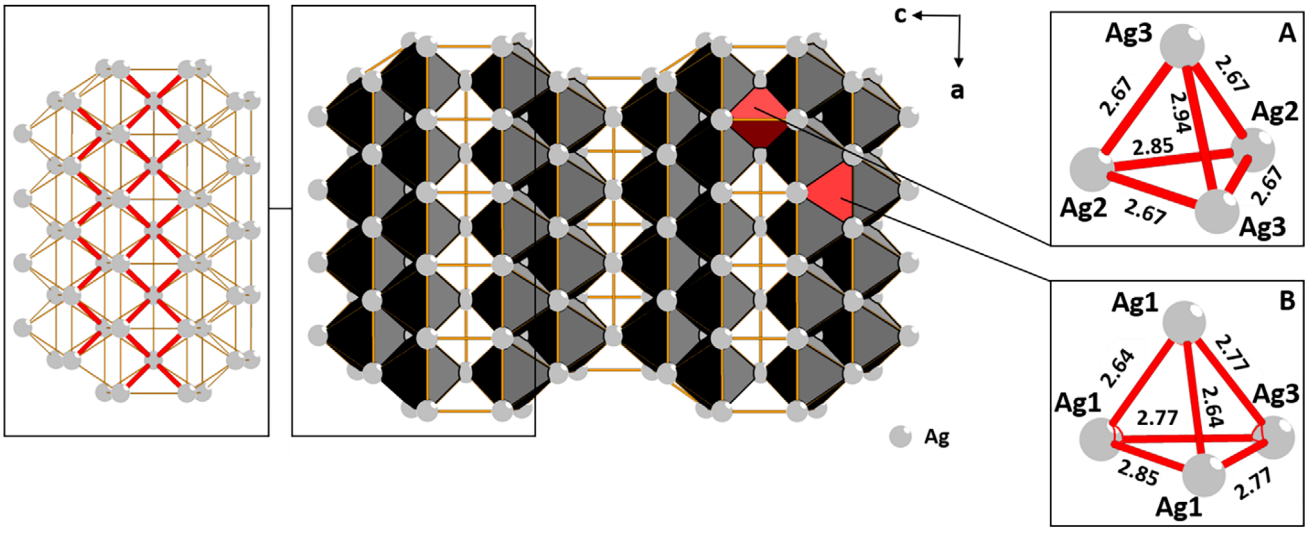

Figure 4. Ag substructure of the crystal structure of $Ag_5Pd_2O_4$ (*Cmcm*, for the complete structure see Figure S3 in Supporting Information) with bond length in Å (without standard deviations for better visibility). For complete data, see Supporting Information. Highlighted in red are the shortest Ag-Ag distances.

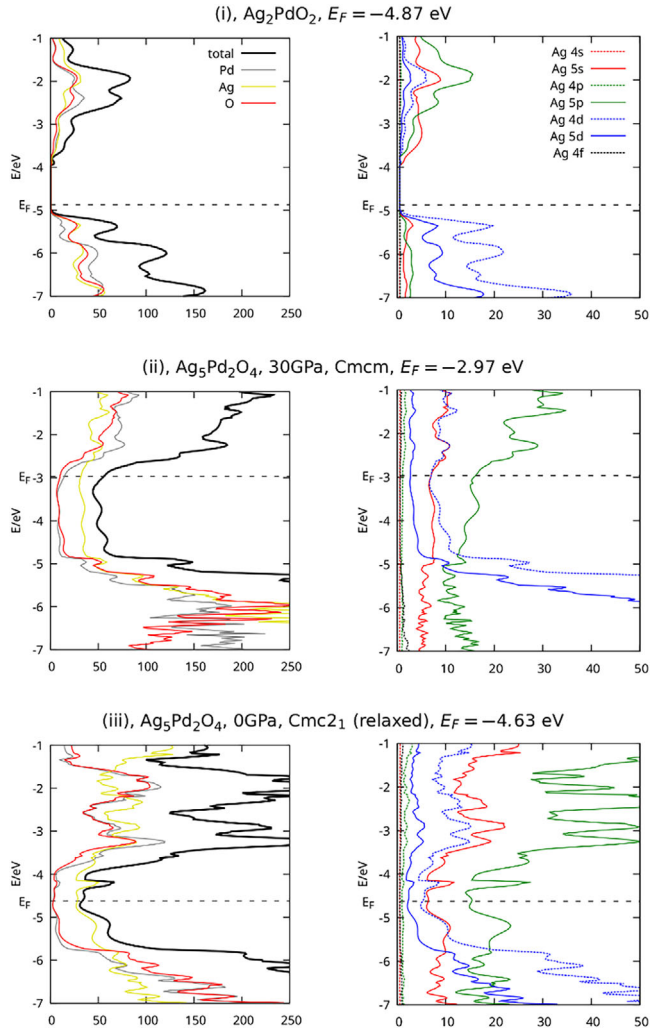

Figure 5. Density of states (DOS) for Ag_2PdO_2 (i), $Ag_5Pd_2O_4$ under pressure (ii) and decompressed (iii), including the Fermi energy (E_F) in the column captions. The graphs in the left column show the total DOS and projections (pDOS) to atoms, and in the right column the pDOS to specific orbitals on silver atoms. Abscissa: relative DOS.

For Ag_2PdO_2, which serves as an example of closed-shell-type silver(I) oxometalates, the DOS and pDOS Figure 5, (i) show a distinct band gap confirming a regular electron count with silver in the integral valence state of + 1. For both the 30.4 GPa (ii) and the decompressed (iii) modifications of $Ag_5Pd_2O_4$, the gap has vanished (total DOS, black lines) and is populated with density on the silver atoms (pDOS, yellow lines). A further projection to individual orbitals on silver, rows (II) and (III), right graphics, of these densities shows it to be made up by mostly 5s and 5p electrons. This fully agrees with our expectations for this kind of system as addressed in the discussion of the crystal structures above and provides independent evidence for the subvalent nature of silver in these configurations.

Even being aware that the accuracy of the simultaneous measurement of the quantum mechanical observables location (by projection to atoms or specific orbitals) and energy (the ordinate in the DOS plots) is limited due to uncertainty, it appears worthwhile to further elaborate on the silver-silver bonding. First indications can be obtained from the energy range covered by the excess silver 5s and 5p pDOS, which is slightly wider for the *Cmcm* than for the $Cmc2_1$ structure, pointing to an enhanced spread in respective binding energies. However, analyzing the distribution of electron density in real space would provide a more persuasive argument in assigning the electron localizations to the contracted Ag-Ag separations in the *Cmcm* crystal structure. Indeed, such accumulations of electron densities associated with the regions of reduced Ag-Ag distances are present. Due to the low number of electrons affected, these are weak but clearly noticeable; see Figure. 5.

3. Conclusions

The first subvalent binary and ternary silver oxides discovered were regarded as exotic singularities with bonding schemes that are hard to classify within the framework of standard models. Meanwhile, a considerable number of further representatives have been synthesized and characterized, hence rendering this phenomenon a general feature of the chemistry of silver.[2]

Unfortunately, discovery of such subvalent silver oxides has so far happened in a rather erratic fashion, and it has proven impossible to identify any systematics with respect to favorable synthesis conditions or element combinations. Now, we have uncovered a new, more targeted approach to the synthesis of subvalent silver oxides by subjecting ternary oxides of monovalent silver to hydrostatic pressure, which enforces phase separation and formation of oxides containing silver in an oxidation state between 0 and + 1. We demonstrate the procedure at the example of Ag_2PdO_2, which decomposes into subvalent $Ag_5Pd_2O_4$ and PdO when exposed to a pressure of 30.4 GPa in a DAC and to laser heating. The crystal structure shows, like in all other related cases, a distinct separation of the anionic, here poly-oxopalladate, and the silver partial structure. The first coordination spheres of palladium allow to assign the oxidation states + 2 and + 4 in the ratio of 1:1, thus leaving three excess electrons per formula unit when assigning the oxidation state of + 1 to silver. This corresponds to an electron count as expressed by $Ag_5Pd_2O_4{\cdot}3e^-$. The excess electrons are accommodated by a 2D double layer of virtually densely packed silver atoms. The findings appear to reflect a singularity, so far only realized with silver, where d^{10}–d^{10} bonding interactions[1b] in silver-rich oxides provide extended Ag^+ partial structures in position space, giving rise to low-lying empty s- and p-bands in reciprocal space that are suited to accommodate extra electrons, that is, enabling the formation subvalent silver. Since in all these compounds the silver substructures are contracted, the new pressure-driven access to such phases as reported here should be generally applicable. The progress achieved is of particular relevance for both basic research and aspiration for useful functionalities. The former includes the aim of exploring material systems as completely as possible, in particular the objective of understanding the underlying chemical bonding. From the perspective of materials research, the discovery reported opens promising vistas since these materials feature a wide spectrum

in electronic transport phenomena, which, in combination with, for example, open-shell transition metal cations, might provide rich magneto-electronic functionalities.

Supporting Information

Deposition Numbers 2419001 (for *Cmcm*-$Ag_5Pd_2O_4$) and 2419002 (for *Cmc*2_1-$Ag_5Pd_2O_4$) contain the supplementary crystallographic data for this paper. These data are provided free of charge by the joint Cambridge Crystallographic Data Centre and Fachinformationszentrum Karlsruhe Access Structures Service.

The authors have cited additional references within the Supporting Information.[18–22]

Acknowledgments

M. B. acknowledges the support of Deutsche Forschungsgemeinschaft (DFG Emmy-Noether Program project BY112/2–1), the LOEWE Program of the state of Hesse and Johanna Quandt Foundation. We acknowledge DESY (Hamburg, Germany), a member of the Helmholtz Association HGF, for the provision of experimental facilities. Parts of this research were carried out at PETRA 3. Beamtime was allocated for proposal I-20230996.

Open access funding enabled and organized by Projekt DEAL.

Conflict of Interest

The authors declare no conflict of interest.

Data Availability Statement

The data that support the findings of this study are available in the Supporting Information of this article.

Keywords: diamond anvil · high pressure · oxide · subvalent · theory

[1] a) M. Jansen, *J. Less Common Met.* **1980**, *76*, 285; b) M. Jansen, *Angew.Chem.* **1987**, *99*, 1136. c) M. Jansen, *Angew. Chem. Int. Ed. Engl.* **1987**, *26*, 1098. d) H. Schmidbaur, A. Schier, *Angew. Chem.* **2015**,*127*, 756. e) H. Schmidbaur, A. Schier, *Angew. Chem. Int. Ed.* **2015**, *54*, 746.

[2] a) W. Beesk, P. G. Jones, H. Rumpel, E. Schwarzmann, G. M. Sheldrick, *J. Chem. Soc. Chem. Comm.* **1981**, 664. b) M. Jansen, C. Linke, *Angew.Chem.* **1992**, *104*, 618. c) M. Jansen, C. Linke, *Angew. Chem. Int. Ed.* **1992**, *31*, 653;[CrossRef] d) M. Jansen, C. Linke, *Z. Anorg. Allg. Chem.* **1992**, *616*, 95; e) C. Linke, M. Jansen, *Inorg. Chem.* **1994**, *33*, 2614; f) M. Schreyer, M. Jansen, *Angew. Chem.* **2002**, *114*, 665. g) M. Schreyer, M. Jansen, *Angew. Chem. Int. Ed. Engl.* **2002**, *41*, 643; h) H. Yoshida, Y. Muraoka, T. Sörgel, M. Jansen, Z. Hiroi, *Phys. Rev. B* **2006**, *73*, 20408; i) U. Wedig, P. Adler, J. Nuss, H. Modrow, M. Jansen, *Solid State Sci.* **2006**, *8*, 753; j) T. Sörgel, M. Jansen, *J. Solid State Chem.* **2007**, *180*, 8; k) S. Ahlert, W. Klein, O. Jepsen, O. Gunnarsson, O. K. Andersen, M. Jansen, *Angew. Chem.* **2003**, *115*, 4458; l) S. Ahlert, W. Klein, O. Jepsen, O. Gunnarsson, O. Krogh Andersen, M. Jansen, *Angew. Chem. Int. Ed.* **2003**, *42*, 4322;[CrossRef] m) A. Kovalevskiy, C. Yin, J. Nuss, U. Wedig, M. Jansen, *Chem. Sci.* **2020**, *11*, 962; n) G. S. Thakur, R. Dinnebier, T. C. Hansen, W. Assenmacher, C. Felser, M. Jansen, *Angew. Chem.* **2020**, *132*, 20082. o) G. S. Thakur, R. Dinnebier, T. C. Hansen, W. Assenmacher, C. Felser, M. Jansen, *Angew. Chem. Int. Ed.* **2020**, *59*, 19910; p) J. Nuss, U. Wedig, M. Jansen, *Z. Anorg. Allg. Chem.* **2022**, *648*, e202200269; q) T. Masese, G. M. Kanyolo, Y. Miyazaki, M. Ito, N. Taguchi, J.: Rizell, S. Tachibana, K. Tada, Z.-D. Huang, A. H. Alshehabi Ubukata, K. Kubota, K. Yoshii, H. Senoh, C. Tassel, Y. Orikasa, H. Kageyama, T. Saito, *Adv. Sci.* **2023**, *10*, 2204672; r) G.: M. Kanyolo, T. Maese, *Mater. Today Phys.* **2023**, *39*, 101271.

[3] M. Schreyer, M. Jansen, *Solid State Sci.* **2001**, *30*, 25.

[4] W. Biltz, *Raumchemie der festen Stoffe", Verlag von Leopold Voss*, Leipzig,**1934**.

[5] W. Klein, M. Jansen, *Z. Anorg. Allg. Chem.* **2008**, *634*, 1077.

[6] A. Jayaraman, *Rev. Mod. Phys.* **1983**, *55*, 65.

[7] a) R. Wolf, R. Hoppe, *Z. Anorg. Allg. Chem.* **1986**, *536*, *77*; b) T. Dahmen, P. Rittner, S. Boeger-Seidl, R. Gruehn, *J. Alloys Compd.* **1994**, *216*, 11; c) J. Bruns, T. Klüner, M. S. Wickleder, *Chem. Eur. J.* **2015**, *21*, *3*, 1294; d) M. S. Wickleder, F. Gerlach, S. Gegelmann, J. Bruns, M. Fenske, K. Al-Shamery, *Angew. Chem.* **2012**, *124*, 2242. e) M. S. Wickleder, F. Gerlach, S. Gagelmann, J. Bruns, M. Fenske, K. Al-Shamery, *Angew.Chem. Int. Ed.* **2012**, *51*, 2199. f) M. Zoller, J. Bruns, G. Heymann, K. Wurst, H. Huppertz, *Z. Naturforsch. B* **2019**, *74*, 381.

[8] a) Y.-H. Wang, D. Walker, B.-H. Chen, B. A. Scott, *J. Alloys Compd.* **1999** *285*, 98; b) R. V. Panin, N. R: Khasanova, A. M. Abakumov, E. V. Antipov, G. van Tendeloo, W. Schnelle, *J. Solid State Chem.* **2007**, *180*, 1566; c) J. Bruns, D. T. van Gerven Klüner, M. S. Wickleder, *Angew. Chem.* **2016**, *128*, 28, 8253; *Angew. Chem. Int. Ed.* **2016**, *128*, 28, 8121.

[9] a) J. Bruns, M. Eul, R. Poettgen, M. S. Wickleder, *Angew. Chem.* **2012**, *124*, *2247*; *Angew. Chem. Int. Ed.* **2012**, *51*, 2204. b) J. Bruns, O. Niehaus, R. Pöttgen, M. S. Wickleder, *Chem. Eur. J.* **2014**, *20*, 811. c) M. Reehuis, T. Saha-Dasgupta, D. Orosel, J. Nuss, B. Rahaman, B. Keimer, O. K. Andersen, M. Jansen, *Phys. Rev. B* **2012**, 11511–81.

[10] a) M. Bykov, E. Bykova, S. van Smaalen, L. Dubrovinsky, C. McCammon, V. Prakapenka, H.-P. Liermann, *Phys. Rev. B* **2013**, *88*, 014110, b) R. Hemley, J. Ultrahigh Pressure Mineralogy: Physics and Chemistry of the Earth's Deep Interior, Berlin, Boston, De Gruyter, **1998**.

[11] a) A. Lobato, M. A. Salvadó, J. M. Recio, *Chem. Sci.* **2021**,*12*,13588.

[12] a) U. Wedig, M. Jansen, B. Paulus, K. Rosciszewski, P. Sony, *Phys. Rev. B* **2007**, *75*, 205123; b) N. Gaston, B. Paulus, U. Wedig, M. Jansen, *Phys. Rev. Lett.* **2008**, *100*, 226404; c) J. Nuss, U. Wedig, A. Kirfel, M. Jansen, *Z. Anorg. Allg. Chem.* **2010**, *636*, 309.

[13] R. Dovesi, R. Orlando, A. Erba, C. M. Zicovich-Wilson, B. Civalleri, S. Casassa, L. Maschio, M. Ferrabone, M. D. la Pierre, P. D'Arco, Y. Noel, M. Causá, M. Rérat, B. Kirtman, *Int. J. Quantum Chem.* **2014**, *114*, 1287

[14] L. Schimka, J. Harl, G. Kresse, *J. Chem. Phys.* **2011**, *134*, 024116

[15] M. F. Peintinger, D. V. Oliveira, T. Bredow, *J. Comput. Chem.* **2012**, *34*, 451.

[16] D. V. Oliveira, J. Laun, M. F. Peintinger, T. Bredow, *J. Comput. Chem.* **2019**, *40*, 2364.

[17] J. Perdew, A. Ruzsinsky, G. I. Csonka, O. A. Vydrov, G. E. Scuseria, L. A. Constantin, X. Zhou, K. Burke, *Phys. Rev. Lett.* **2008**, *100*, 136406.

Manuscript received: June 12, 2025
Revised manuscript received: August 25, 2025
Version of record online: September 15, 2025